

RECENT ADVANCES AT THE GLOBUS-M2 TOKAMAK

N.N. Bakharev and Globus team

30th IAEA Fusion Energy Conference (IAEA FEC 2025)
Oct 13 – 18, 2025 Tianfu International Convention Center

List of contributors



N.N. BAKHAREV, A.S. ALEXANDROV, S.E. ALEXANDROV, I.M. BALACHENKOV, M.K. BUTS, F.V. CHERNYSHEV, V.V. DYACHENKO, N.V. ERMAKOV, S.V. FILIPPOV, A.N. GOLYAKOV, V.YU. GORYAINOV, E.Z. GUSAKOV, V.K. GUSEV, A.YU. IVANOV, E.M. KHILKEVITCH, N.A. KHROMOV, E.O. KISELEV, A.N. KOVAL, A.N. KONOVALOV, S.V. KRIKUNOV, A.K. KRYZHANOVSKY, G.S. KURSKIEV, A.S. MAREEV, O.S. MEDVEDEV, A.D. MELNIK, V.B. MINAEV, I.V. MIROSHNIKOV, E.E. MUKHIN, A.N. NOVOKHATSKY, M.I. PATROV, YU.V. PETROV, A.YU. POPOV, A.G. RAZDOBARIN, N.V. SAKHAROV, A.E. SHEVELEV, P.B. SHCHEGOLEV, K.D. SHULYATIEV, O.M. SKREKEL, V.V. SOLOKHA, A.YU. TELNOVA, N.V. TEPOLOVA, E.E. TKACHENKO, V.A. TOKAREV, S.YU. TOLSTYAKOV, G.A. TROSHIN, E.A. TYUKHMENEVA, V.I. VARFOLOMEEV, N.S. ZHILTSOV

Ioffe Institute

St.-Petersburg, Russia

Email: bakharev@mail.ioffe.ru

E.G. KAVEEVA, K.A. KUKUSHKIN, A.M. PONOMARENKO, V.A. ROZHANSKY, I.YU. SENICHENKOV, A.Y. TOKAREV, A.Y. YASHIN
Peter the Great St. Petersburg Polytechnic University
St.-Petersburg, Russia

A.V. BONDAR, E.N. BONDARCHUK, A.A. KAVIN, I.V. KEDROV, A.B. MINEEV, V.N. TANCHUK, V.A. TROFIMOV, A.A. VORONOVA
JSC «NIIefa»
St.-Petersburg, Russia

P.A. BAGRYANSKY, S.V. IVANENKO, A.D. KHILCHENKO, A.N. KVASHNIN, E.I. PINZHENIN, I.V. SHIKHOVTSEV, A.L. SOLOMAKHIN
Budker Institute of Nuclear Physics
Novosibirsk, Russia

A.S. DZHURIK, YU.A. KASHCHUK, S.YU. OBUDOVSKY
Project Center ITER
Moscow, Russia

E.G. ZHILIN
Ioffe Fusion Technology Ltd.
St.-Petersburg, Russia

A.E. KONKOV, P.S. KORENEV
V.A. Trapeznikov Institute of Control Sciences of Russian Academy of Sciences, Moscow, Russia

V.A. SOLOVEY
B.P. Konstantinov Petersburg Nuclear Physics Institute, Kurchatov Institute
St. Petersburg, Russia



- **Introduction**
- **Wall conditioning**
 - Inter-Shot boronization
 - In-situ wall diagnostics
- **Confinement & heating**
 - Hot ion mode during NBI
 - ICRH
- **SOL**
 - High field side high density
 - Power decay length
- **Instabilities**
 - Alfvén Instabilities
 - ELMs
- **Globus-3**
- **Conclusion**

Globus-M2

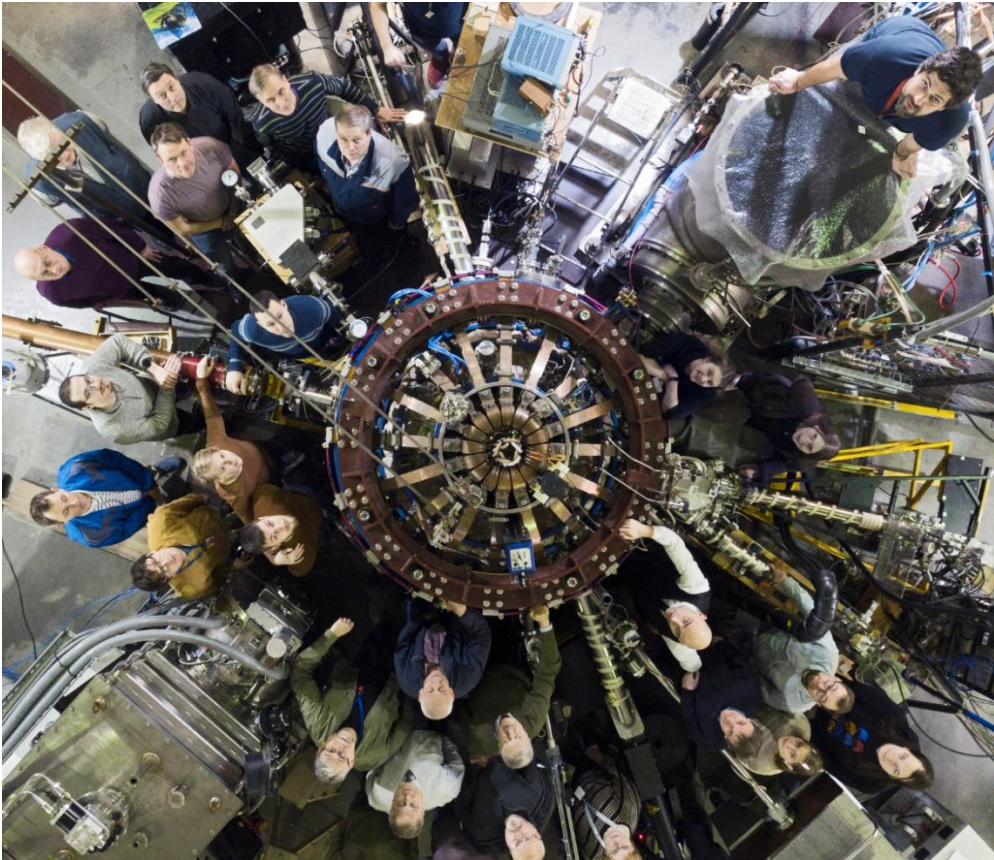


Parameter	Value design/achieved
R [cm]/a [cm]	36/24 = 1.5
k	2.0/2.1
δ	0.5/0.4
B _T [T]	1/0.95
I _p [kA]	500/450
t _{pulse} [ms]	400/170
E _{NBI} [keV]	30-50
P _{NBI} [MW]	2/2
Max T _i , [keV]	4.7 at $\langle n_e \rangle_i = 5 \cdot 10^{19} \text{ m}^{-3}$
Max T _e [keV]	1.8 at $\langle n_e \rangle_i = 5 \cdot 10^{19} \text{ m}^{-3}$

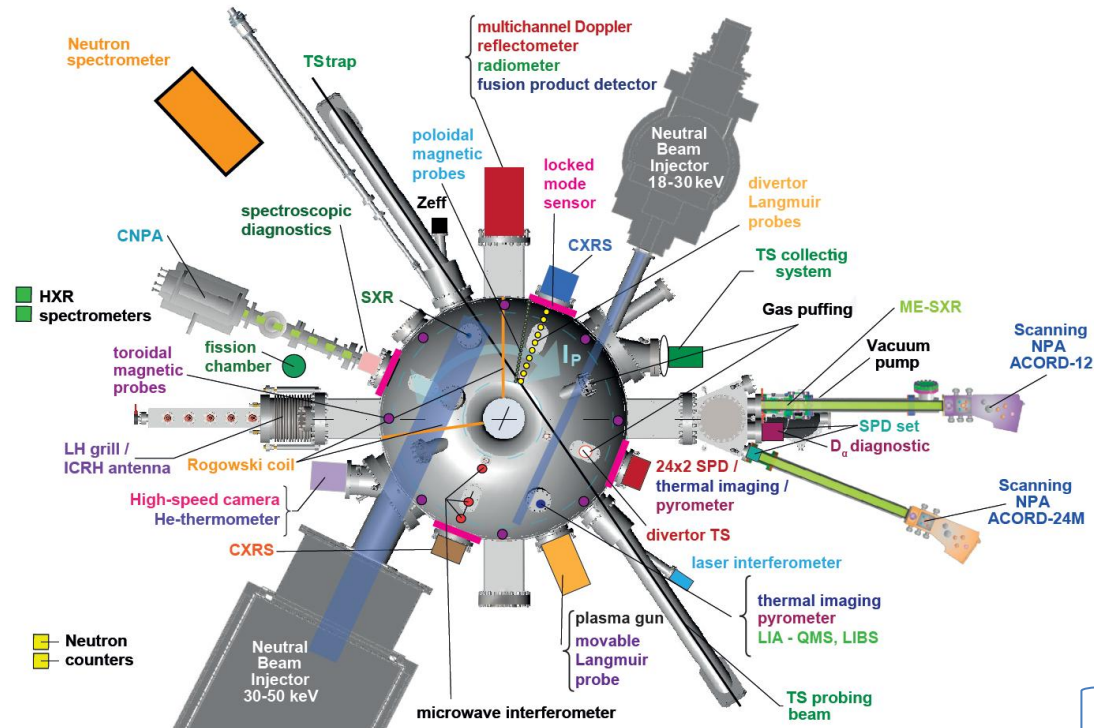
Extreme specific heating power $\approx 4 \text{ MW/m}^3$

Additional systems:

2.45 GHz LHCD, 5-15 MHz ICRH



Diagnostics Development



ITER
technologies

- dispersion interferometer

[IVANENKO, S.V. et. al., Fus. Eng. Des. 202 (2024) 114409]

- charged fusion product detector

[BAKHAREV, N. N., et al. Tech. Phys. Lett. 50 10 (2024) 24-27.]

- two-color pyrometer

[VORONIN, A. V., et al. Tech. Phys. 68 12 (2023) 799-805],

- locked-mode sensor

[PETROV, Y. V., et al., Plasma Phys. Rep.. 50 7 (2024) 773-780.]

- high-speed cameras [TIMOKHIN, V., EX-E P4]

- Silicon Precision Detector array

- Real time Plasma EQ and control

(under implementation)

[KORENEV, P. S., et al. Tech. Phys. Lett. 49 4 (2023) 372-375.]

- LIA-QMS, LIBS

[RAZDOBARIN, A.G. et al. Plasma Phys. Rep. 50 6 (2024) 667–677][O.S. MEDVEDEV, et al., Nucl. Mater. and Energy. 41 (2024) 101829.]

- U^{235} neutron cameras

[KORMILITSYN TEC-FNT, P6]

- Divertor Thomson Scattering

[ERMAKOV, N. V., et al., Plasma Phys. Rep. 49 12 (2023) 1480]

Inter-Shot Boronization (ISB)



New boronization technique was utilized during the 2024-2025 campaign.

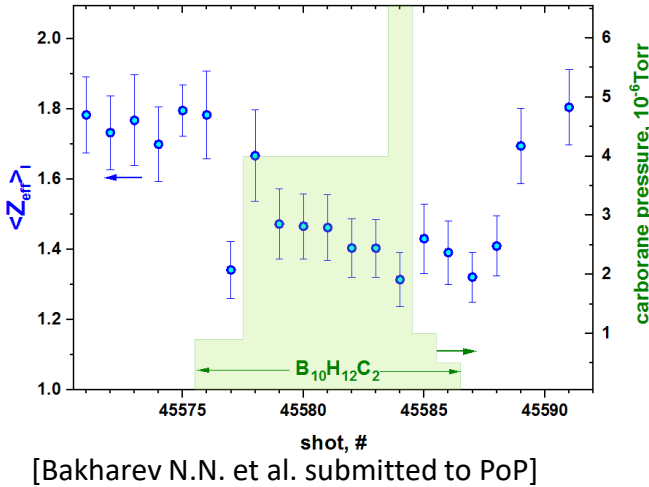
Significant advantage over conventional glow discharge boronization (GDB)

Technique:

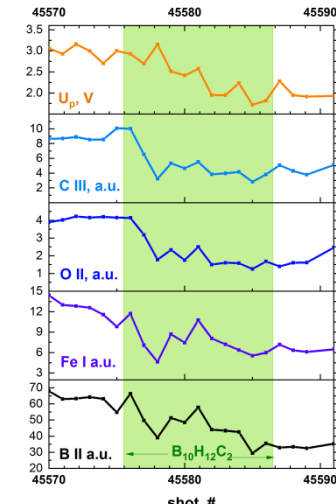
- vessel with carborane ($B_{10}H_{12}C_2$) connected to tokamak – gas inflow between shots.
- Boronization is happening in the initial phase of the discharge->doesn't affect plateau

Z_{eff} decreases during ISB

$\langle n_e \rangle = 2 \times 10^{19} \text{ m}^{-3}$, before sawtooth start

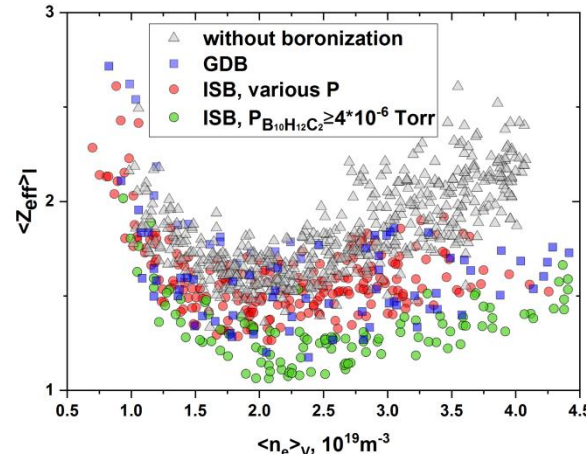


U_p , and impurity lines demonstrate similar behaviour.



$Z_{\text{eff}} < 1.1$ during NBI in C-wall tokamak

$B_T = 0.7-0.8 \text{ T}$, $I_p = 300 \text{ kA}$, $P_{\text{NBI}} = 700 \text{ kW}$, 40 keV D NBI

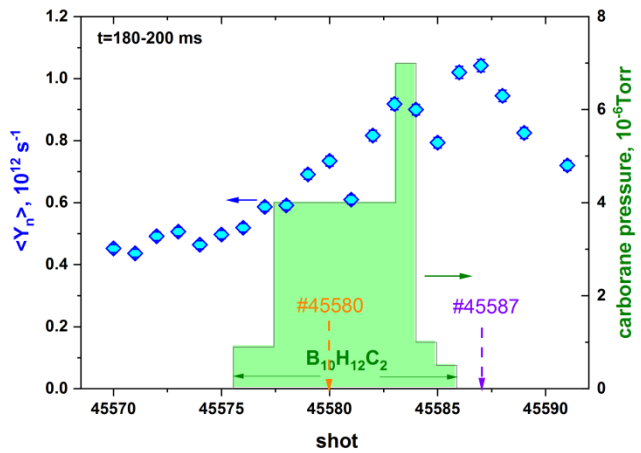


Inter-Shot Boronization (ISB)



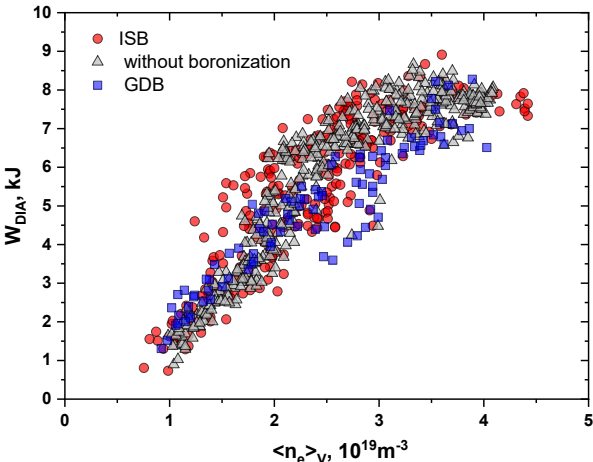
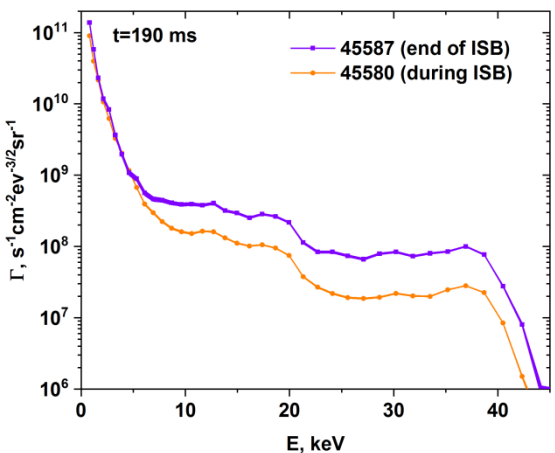
DD Neutron rate doubling

While NUBEAM modeling predict neutron rate decrease



Fast ion confinement improvement

NPA energy spectra:



For the same n_e #41570 vs #41580:

- NUBEAM simulation: 30% Y_n decrease
- Experiment: 60% Y_n increase

Most probable explanation: decrease of Charge-Exchange losses

No energy confinement change

As compared to the case without boronization
 $\tau_E \sim 12$ ms ($\langle n_e \rangle_V \approx 3 \cdot 10^{19} \text{ m}^{-3}$) is consistent with
 Glb-21 scaling

3D localized in-situ co-deposition study

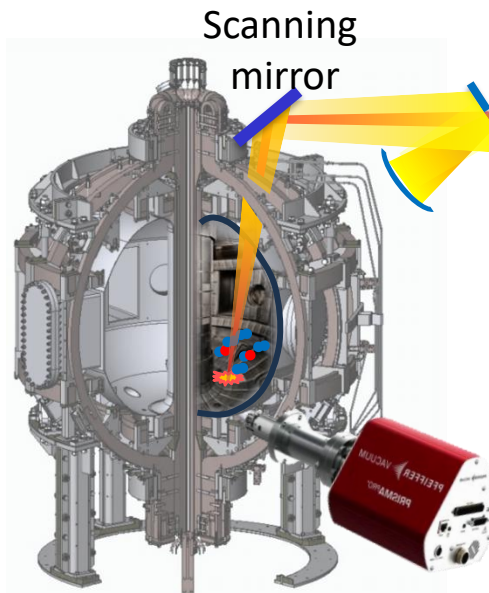


LIA-QMS (Laser-Induced Ablation + Quadrupole Mass-Spectrometry) – **in-situ** layer-by layer H/D concentration

LIBS (Laser-Induced Breakdown Spectroscopy)-Elemental composition with ~500 nm depth resolution

[RAZDOBARIN, A.G. et al. Plasma Phys. Rep. **50** 6 (2024) 667–677]

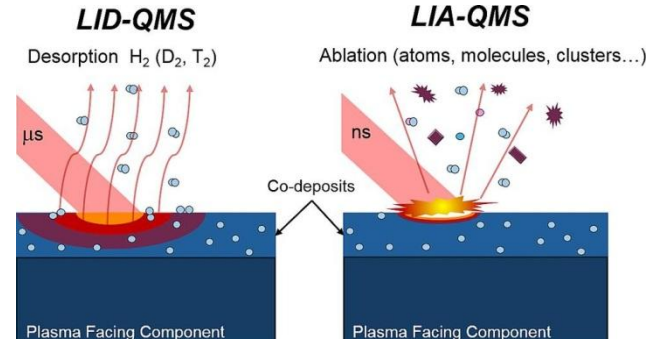
[O.S. MEDVEDEV, et al., Nucl. Mater. and Energy. **41** (2024) 101829.]



Nd:YAG laser
1064 nm, 9 ns
5-10 J/cm²

Residual gas analyzer –
QMS

- 1) Optical spectroscopy (LIBS)
Wideband spectrometer 250-750 nm
for elemental analysis
- 2) High resolution spectrometer 655-657 nm
for hydrogen isotopes separation

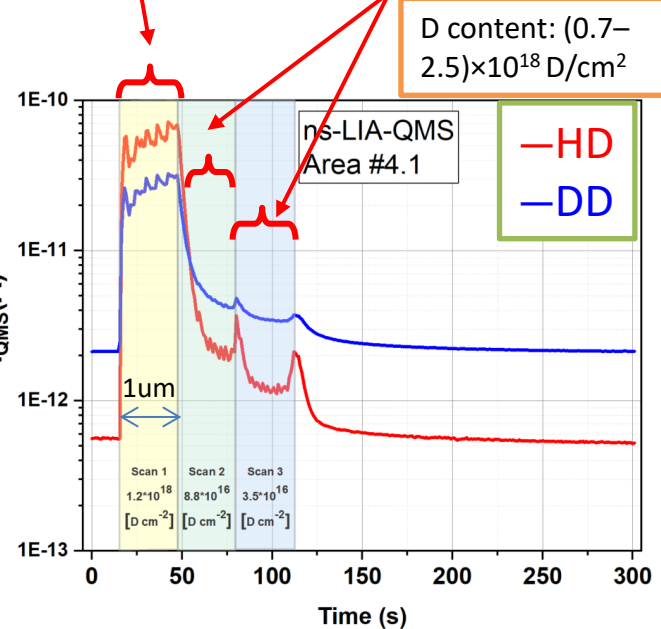


3D localized in-situ co-deposition study



In-situ LIA-QMS

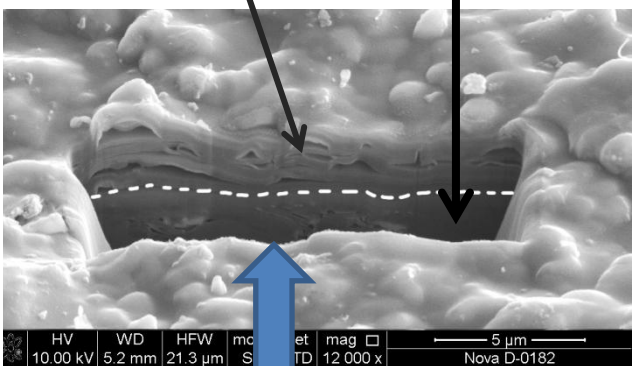
In divertor



Post mortem FIB-SEM

Co-deposition

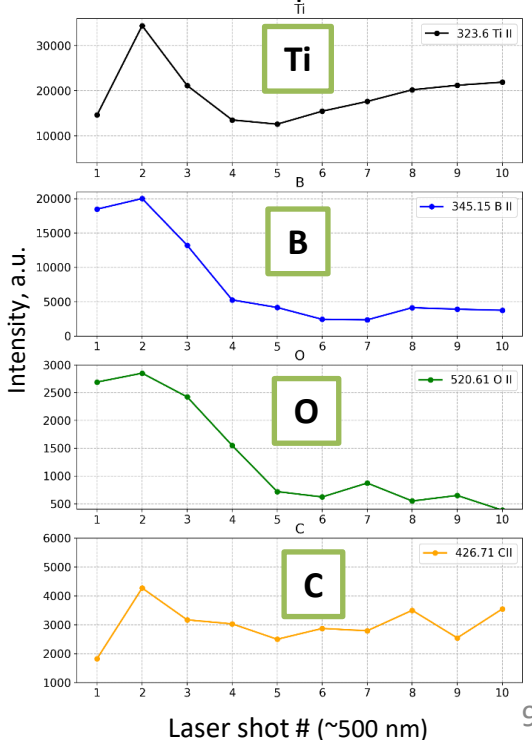
carbon



FIB trench in the C tile

In-situ LIBS in vacuum

Qualitative layer-by-layer elemental composition





Confinement: Hot Ion Mode

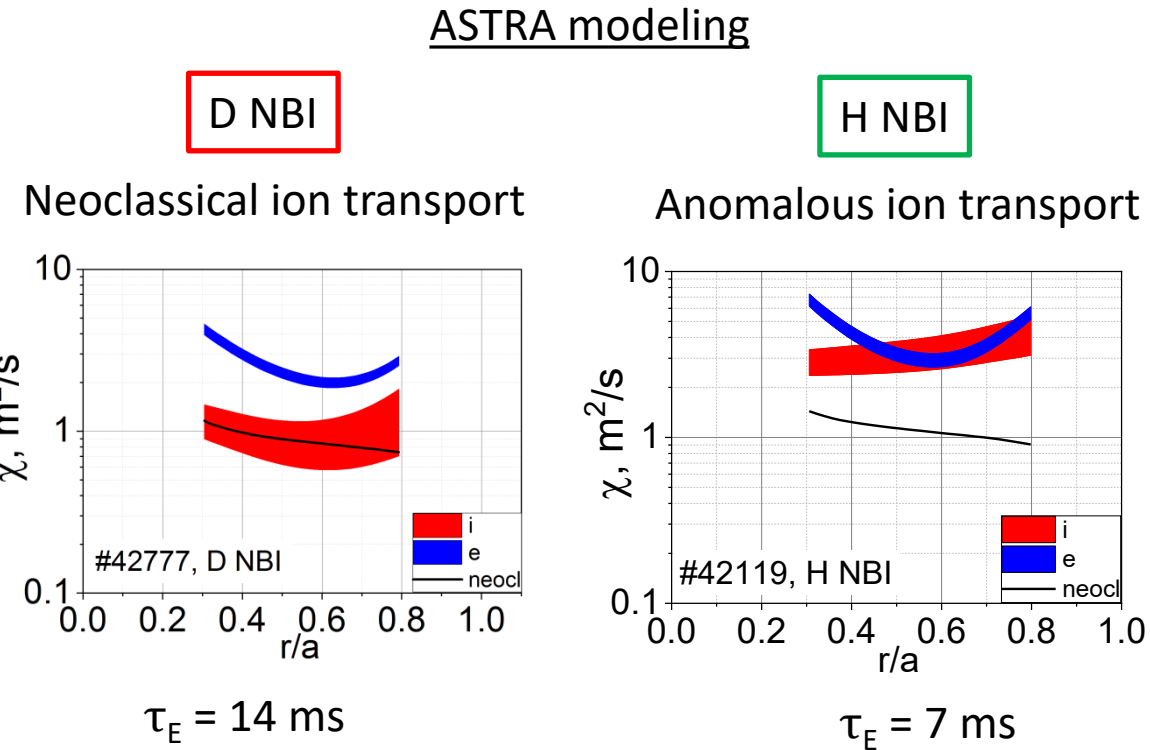
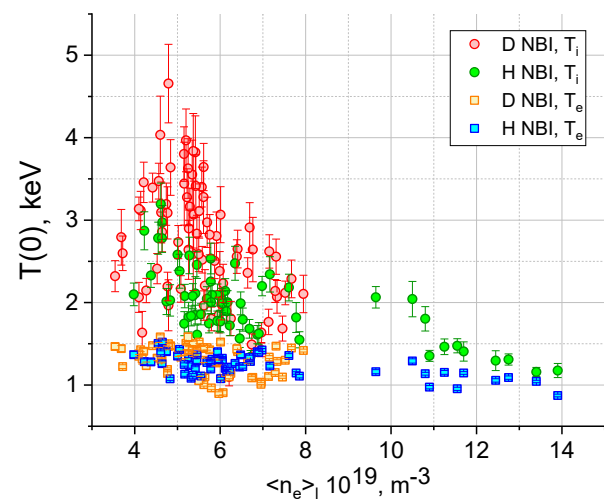
Hot-ion mode - a natural operating regime of Globus-M2
during H and D NBI in D plasma at $B_T \geq 0.7$ T

[KURSKIEV, G.S., EX-H P4]

[G. S. Kurskiew et al. Plasma Phys. Rep. 49, 403–418 (2023)]

MAX $T_i(0)$
D NBI: 4.7 keV
H NBI: 2.9 keV

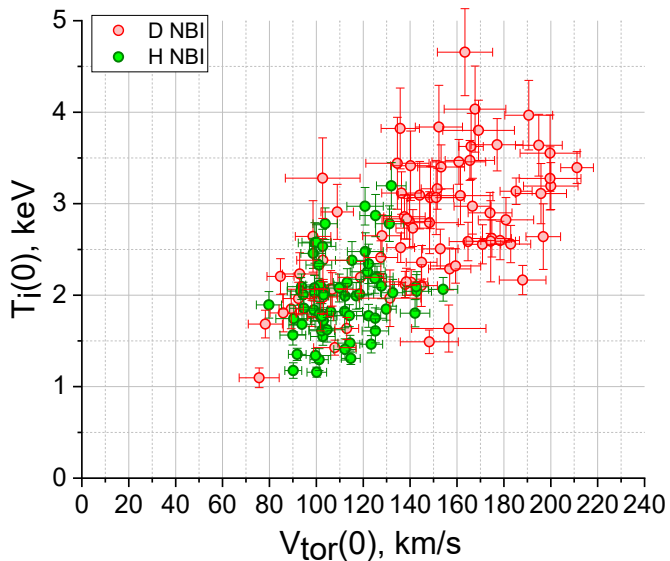
$B_T = 0.8\text{--}0.9$ T
 $I_p = 300\text{--}400$ kA



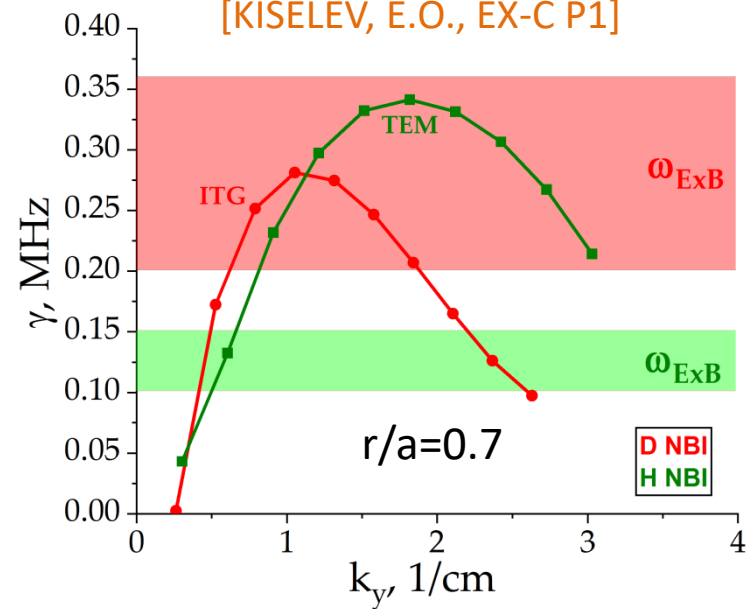


Confinement: Hot Ion Mode

Higher T_i corresponds to higher rotation velocity



Linear gyrokinetic simulation with GENE
[KISELEV, E.O., EX-C P1]



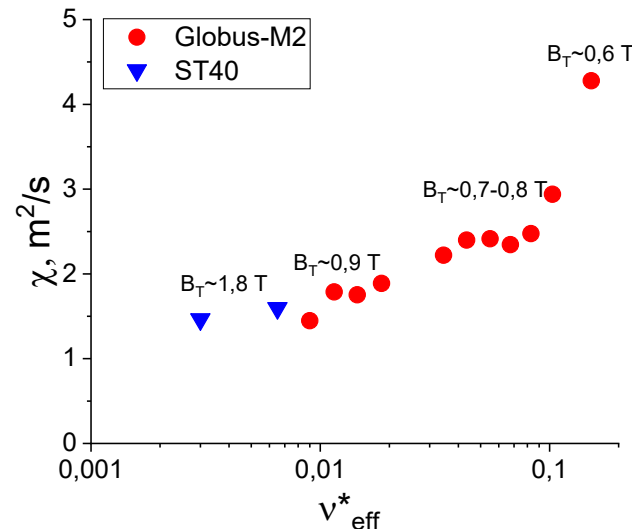
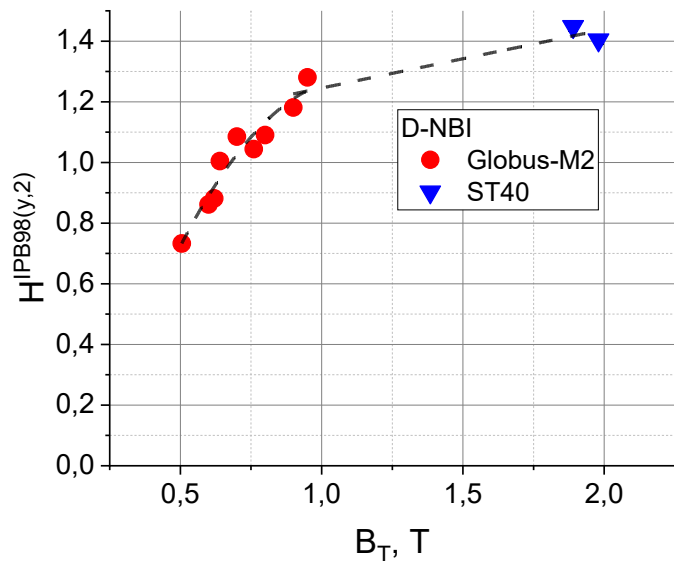
ITG is suppressed by the rotation velocity shear during D NBI
During H NBI rotation is not enough to suppress TEM

Confinement: Hot Ion Mode



Previous ST data had suggested a strong confinement improvement with B_T increase

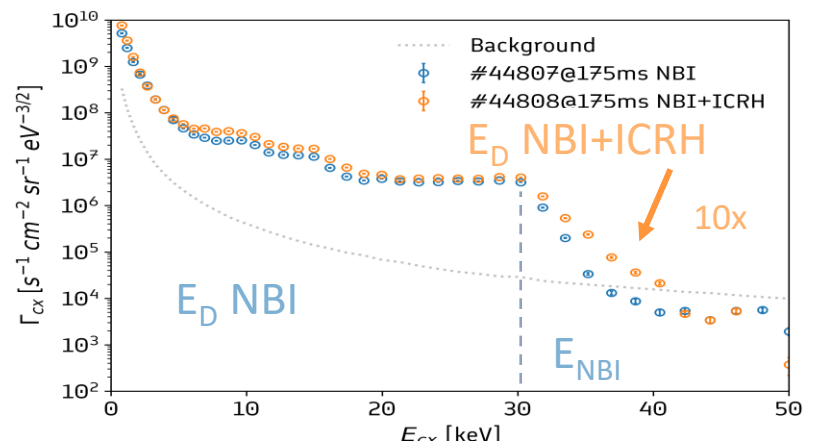
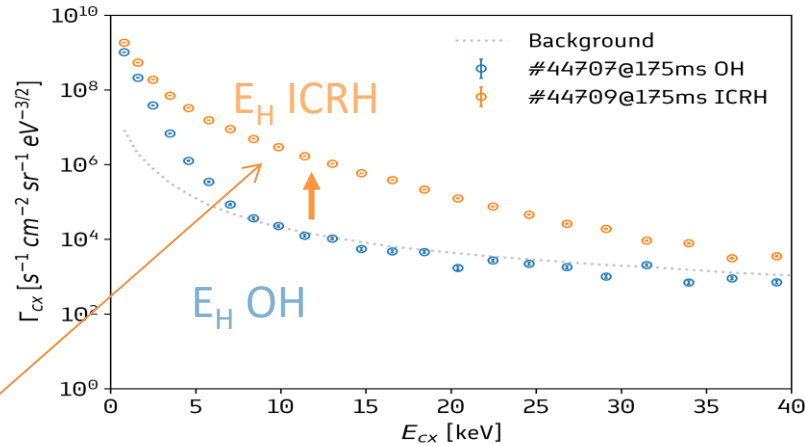
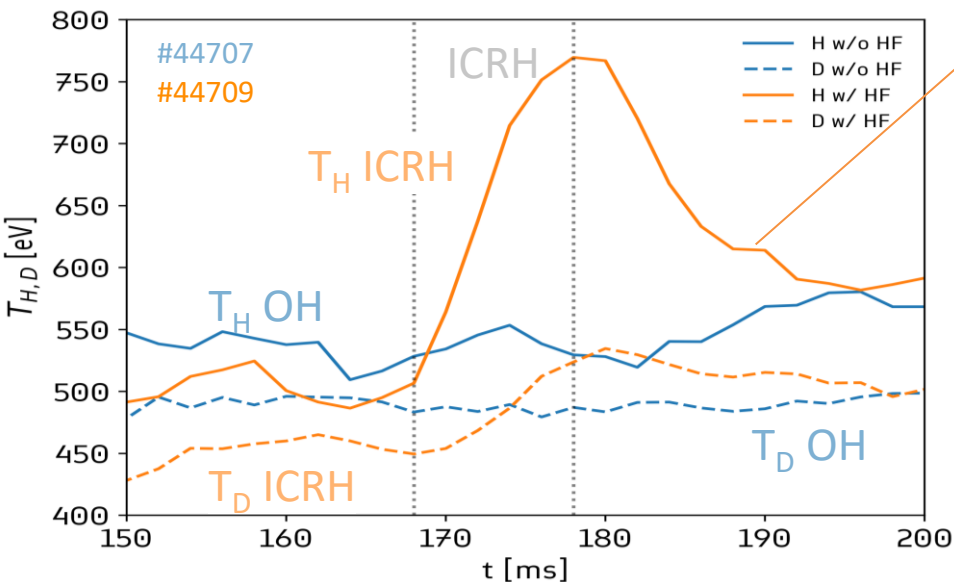
Data from Globus-M/M2 and ST-40 data [MCNAMARA, S. A. et al. Nucl. Fusion. **63** 5 (2023) 054002][KAYE, S. M., et al. PPCF **65** 9 (2023) 095012]



New data indicate saturation of confinement improvement at $B_T \sim 1 T$.

Confinement: ICRH

During Globus-M2 2024 campaign the novel experiments with ICRH in Minority Heating and 2nd harmonic regimes at $B_T=0.7$ T. Absorbed power ~ 50 kW.
 MH experiments exhibited 15% increase in T_i at $X_H \sim 20\%$. . .
 2nd harm. NBI+ICRH showed 10x growth of n^D with $E > E_{NBI}$



HFSHD

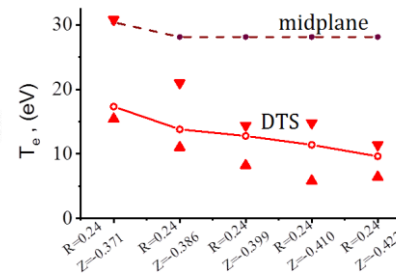
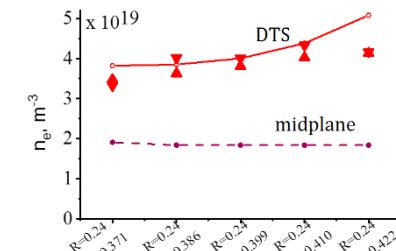
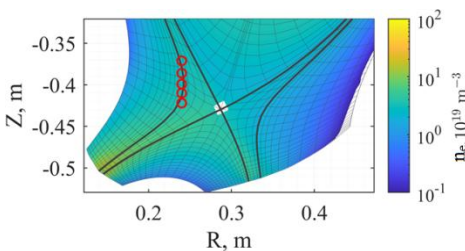


High Field Side High Density feature has been discovered in Globus-M2 using newly installed divertor Thomson scattering

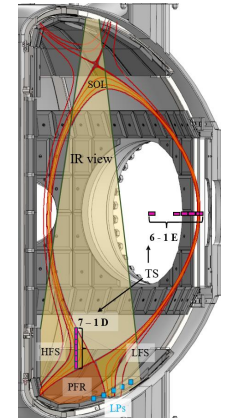
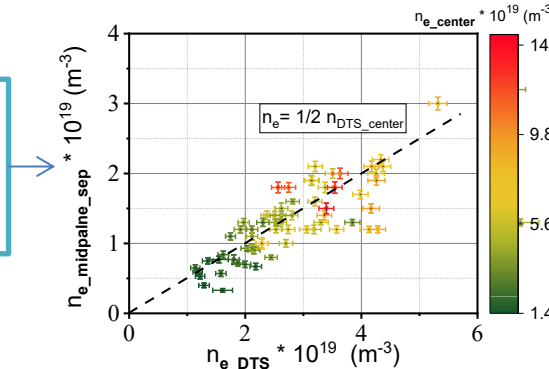
[E.E. Mukhin, EX-D, P2]

Observed over a wide range of discharge parameters: $n_e(0)$: $2 \cdot 10^{19}$ - $1.4 \cdot 10^{20} \text{ m}^{-3}$
with and without NBI

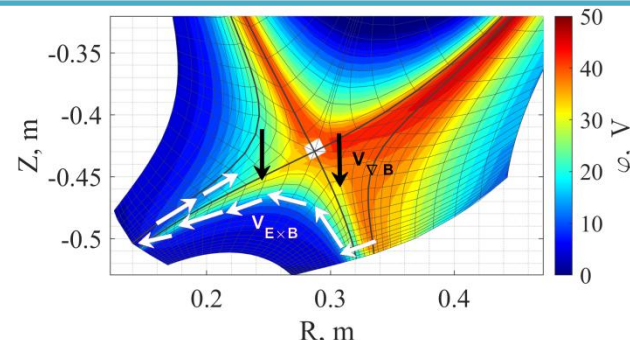
SOLPS-ITER simulation taking into account drifts experiment



n_e at the inner divertor leg
1.5-3x higher than in midplane



ExB drift in the HFS direction leads to the formation of a HFSHD



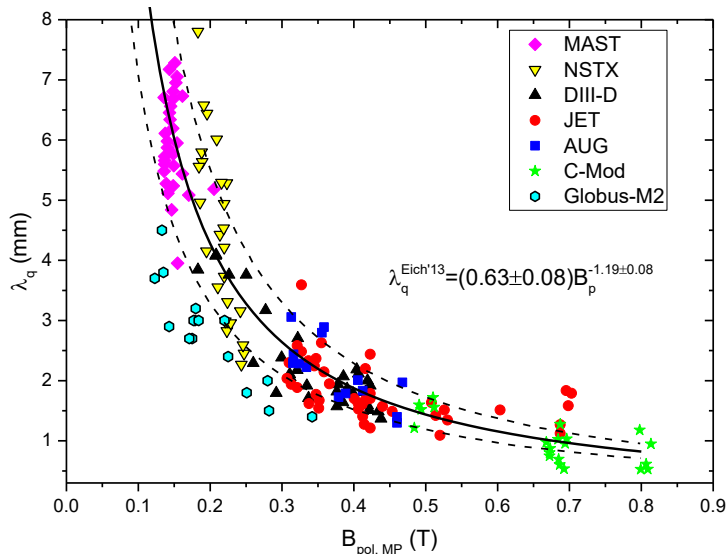
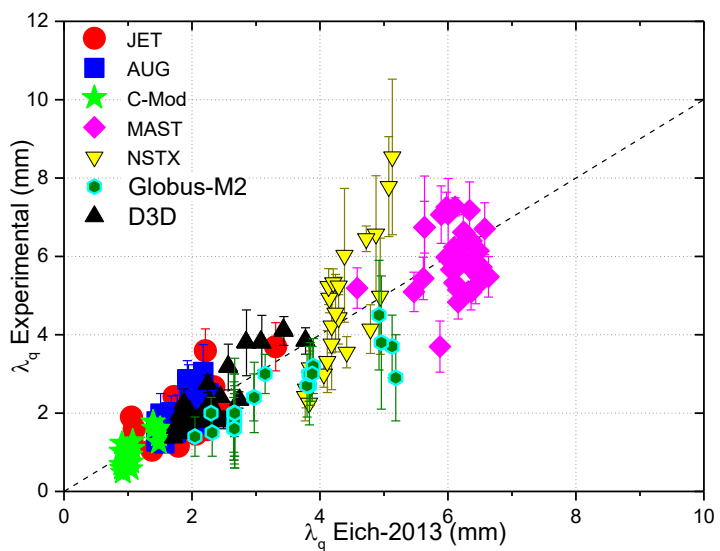
The total drift flux through the inner divertor separatrix equals to approximately 50% of the ion flux to the inner target

SOL power decay length



SOL power decay length λ_q was measured using IR thermography
 $B_T=0.5\text{-}0.95\text{ T}$, $I_p=155\text{-}400\text{ kA}$, up to 0.8 MW NBI

Comparison with multi-machine scaling

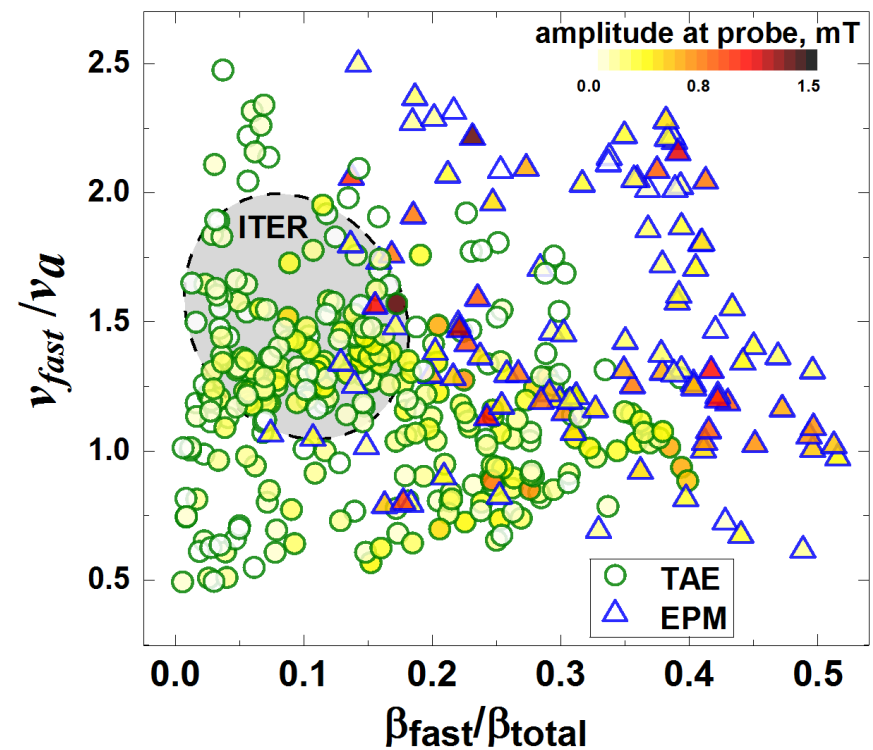


$\lambda_q \sim B_p^{-1}$ in ST with B_T up to 0.95 T and $\lambda_q \sim 2\text{mm}$,
 confirming data from conventional devices ($\lambda_q \sim B_p^{-1.19}$)

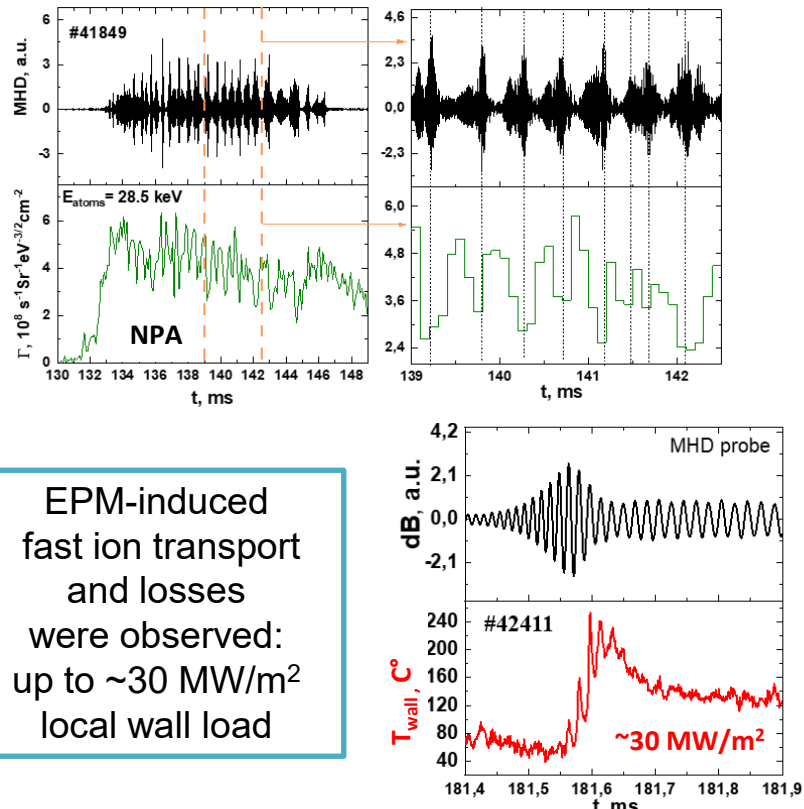
Alfvén Instabilities



Alfvén-type instabilities exists
in a wide range of experimental parameters



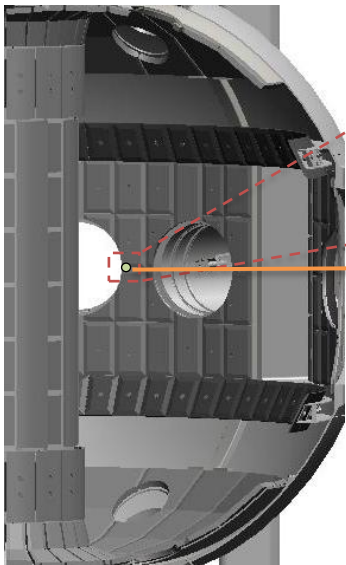
Improved plasma parameters and fast-ion confinement ⇒
previously unobserved **EPMs**



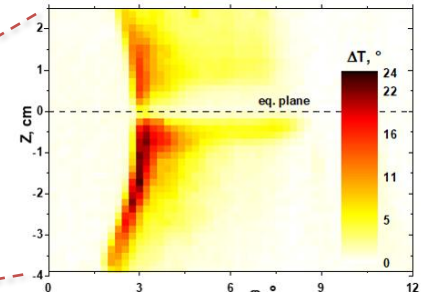
Alfvén Instabilities: TAE



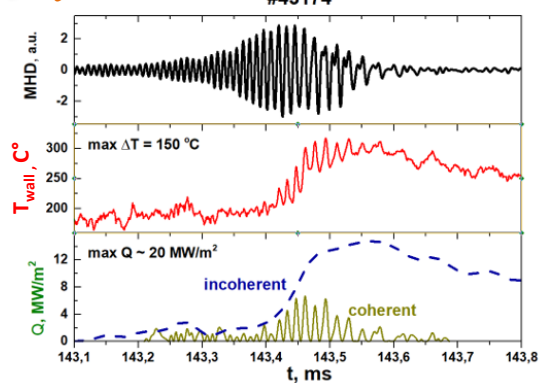
Up to **20 MW/m²** local fast ion wall load during **TAE** was observed



IR camera

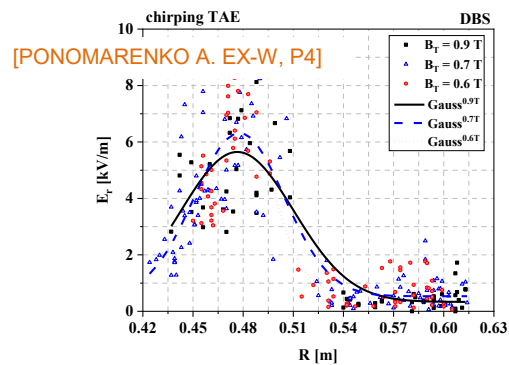


Pyrometer

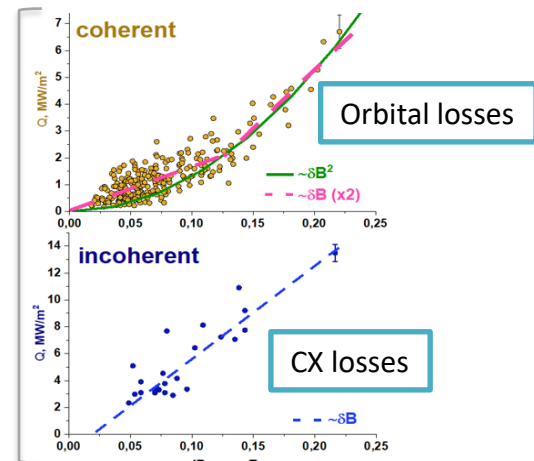


[SKREKEL O.M. EX-W, P4]

Multi-frequency Doppler backscattering method demonstrated central localization



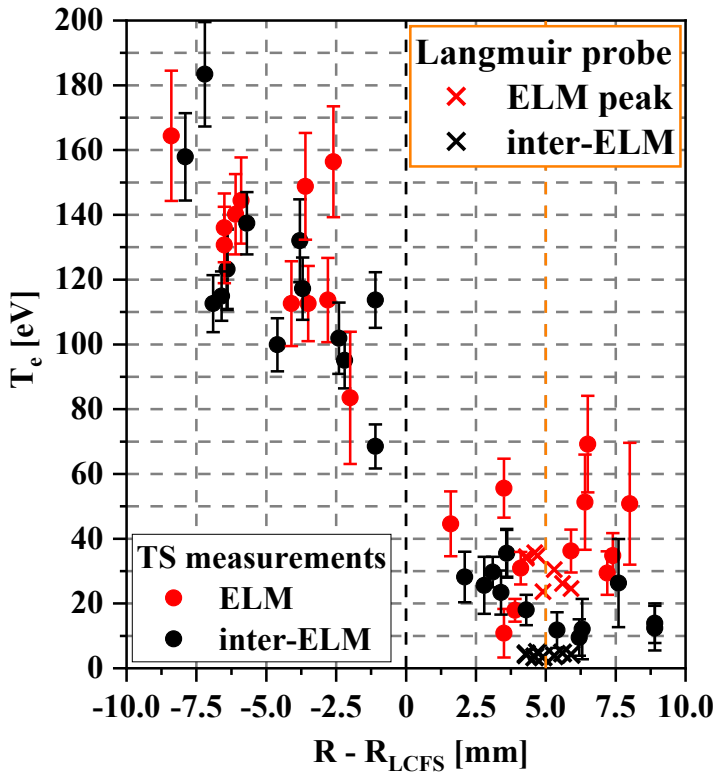
[PONOMARENKO A. EX-W, P4]



Both **coherent** and **incoherent** components are associated with the **convective transport** but different type of losses: **orbital** and **CX** respectively.

ELMS

During small ELMs significant T_e changes inside the separatrix were not observed

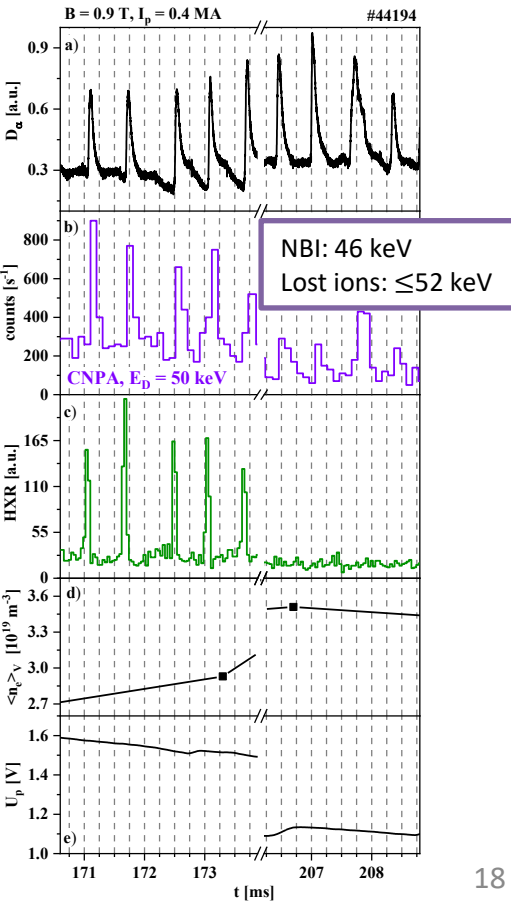


Fast particle losses associated with ELMs were found

[A. Ponomarenko et al 2024 Nucl. Fusion 64 022001]

[A.Y. Tokarev et al Plasma Phys. Rep. 50, 541–551 (2024)]

[A. Yashin et al submitted to Physics of Plasmas].



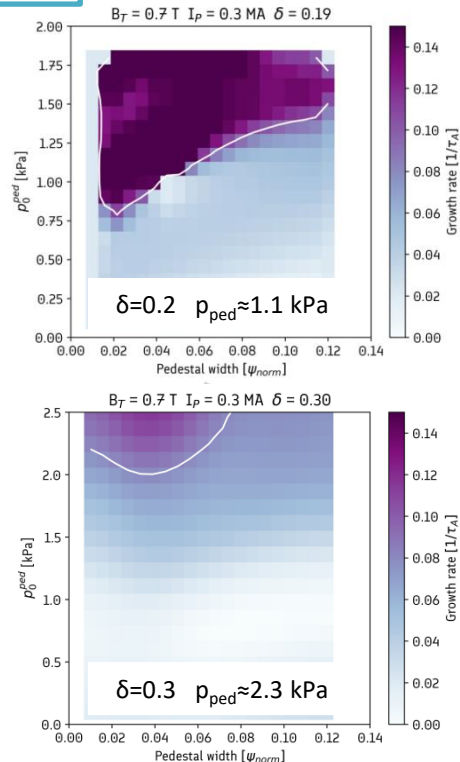
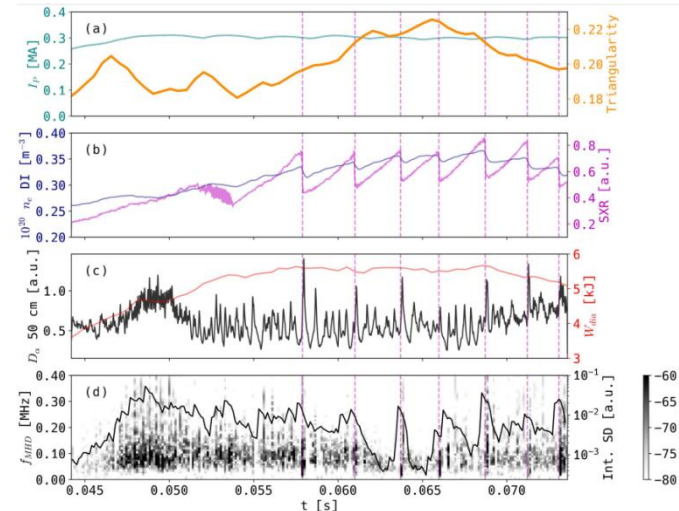
Low triangularity

Triangularity was varied from 0.4 to 0.2

[Solokha V.V. TH-S, P7]

Low triangularity pulses ($\delta=0.2$) exhibited small ELMs at pedestal pressure around 1 kPa

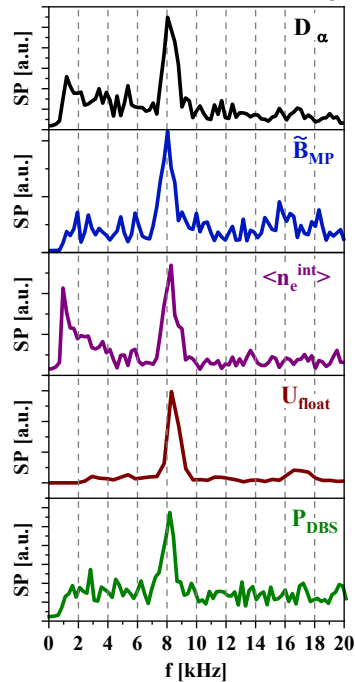
#44330



ELM-free regime with EHO

[Yashin A. Yu. EX-E, P4]

#44335 EHO



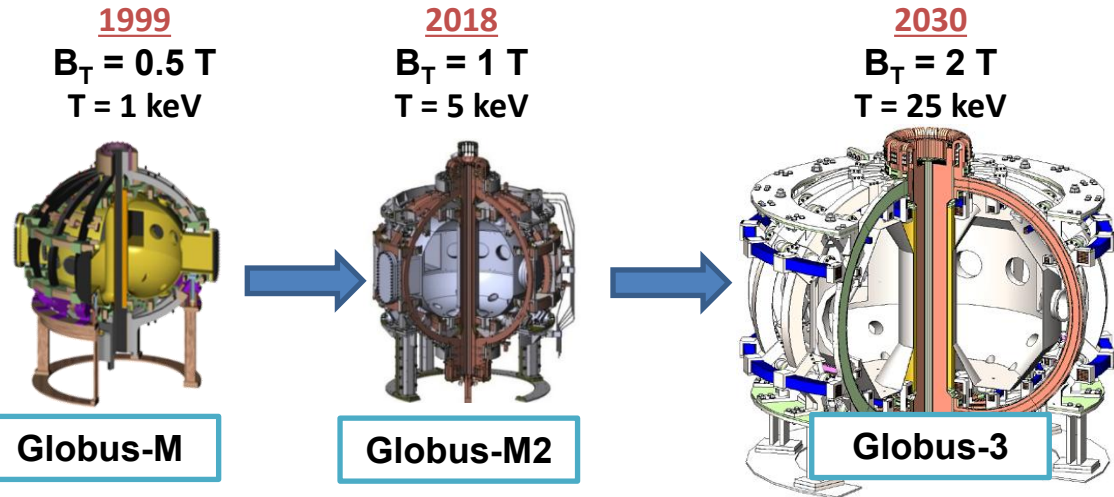
The 3-field linear MHD simulations using BOUT++ showed low- δ PB to have peeling traits and mode structure located near separatrix, while mid- δ PB have more ballooning properties and wider structure.





Globus-3

Globus-3 is the next step ST in Ioffe institute. [Minaev V.B. PWF-P2]



- Design implements Globus-M and Globus-M2 solutions, while correcting their design flaws
- The project is aiming to achieve thermonuclear plasma (simultaneous $T_{i0} \sim 25 \text{ keV}$, $\langle n_e \rangle \sim 10^{20} \text{ m}^{-3}$) in H plasma
- Globus-3 will be a tokamak with the highest $P_{\text{aux}}/V = 3-4 \text{ MW/m}^3$ in the world.

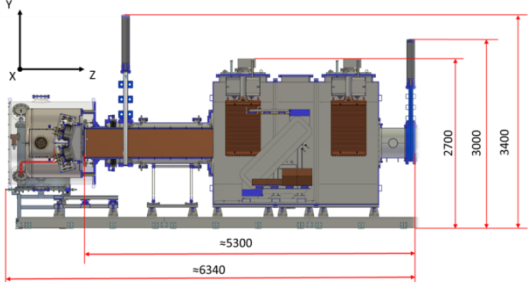
Parameter	Globus-M	Globus-M2	Globus-3
R/a	$0.36/0.24=1.5$		$0.775/0.44=1.76$
B_T, T	0.5	1	2
I_p, MA	0.2	0.5	2
t pulse, s	0.1	0.4	3
NBI, MW	1	2	11.5 (14)

Application of ICRH,
LHCD and ECRH Is
under consideration.

Globus-3



Continuous delivery of 2-3xNBI from Budker institute



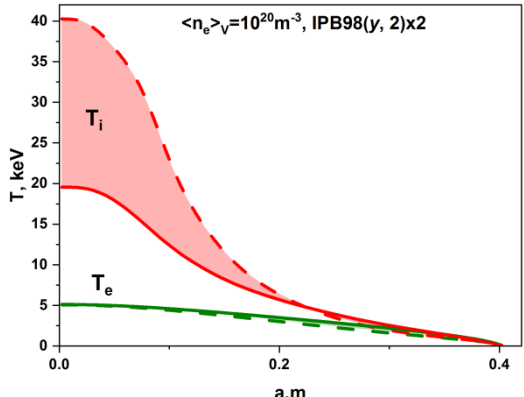
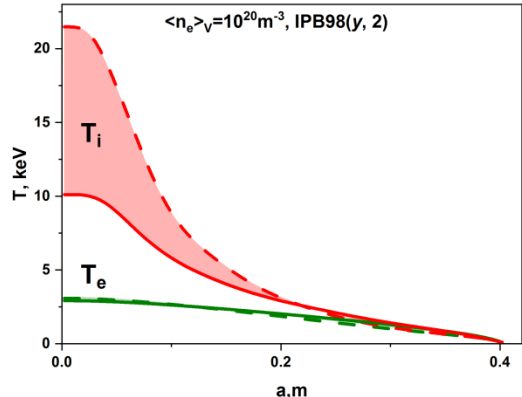
$$E_{\text{NBI}} = 50-60 \text{ keV}$$

$$P_{\text{NBI}} = 5 \text{ MW}$$

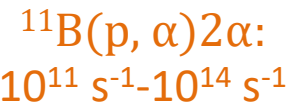
$\langle n_e \rangle_v = 10^{20} \text{ m}^{-3}$, 11.5 MW 60 keV NBI, Hot-ion mode, neoclassical ions

Base scenario,
H-factor=1

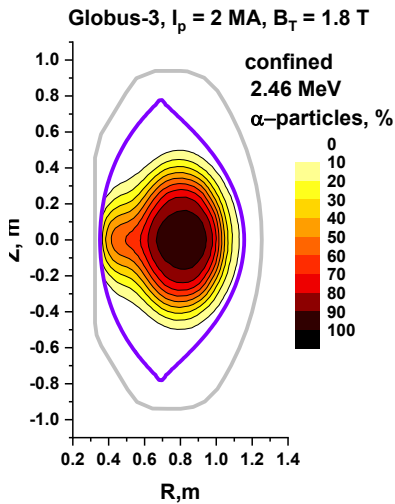
Upside scenario,
H-factor=2



α -particle from



Acceptable for
experimental studies



Timeline:

Conceptual design – 2025 – 2026

Detailed design – 2026 – 2027

Manufacturing of EMS and VV – 2027-2029

Modernization of the power supply system – 2029 – 2031

Assembling the Globus-3 – 2030

Start-up of the tokamak with the existing heating and diagnostics systems - 2031

Conclusion



- Advanced diagnostics and control were successfully implemented
- A novel **Inter-Shot Boronization** technique was demonstrated $Z_{\text{eff}} < 1.1$ the neutron yield doubling.
- A **hot-ion mode** was established as a natural regime for Globus-M2. **D NBI** provides superior ion thermal insulation through **toroidal rotation gradient stabilization of ITG turbulence**.
- **ICRH** experiments demonstrated **15% T_i** increase and beam ion acceleration.
- The **High-Field-Side High-Density** phenomenon was identified for the first time in ST.
- Alfvén eigenmodes cause up to **$\sim 30 \text{ MW/m}^2$ wall load**.
- ELMs were shown to perturb plasma parameters only outside the LCFS but cause fast particle losses.
- The next-generation **Globus-3 ST** is under preliminary design. With significantly increased parameters ($B_T=2 \text{ T}$, $I_p=2 \text{ MA}$, $R=0.775 \text{ m}$) it is projected to achieve **fusion-relevant plasma parameters**.

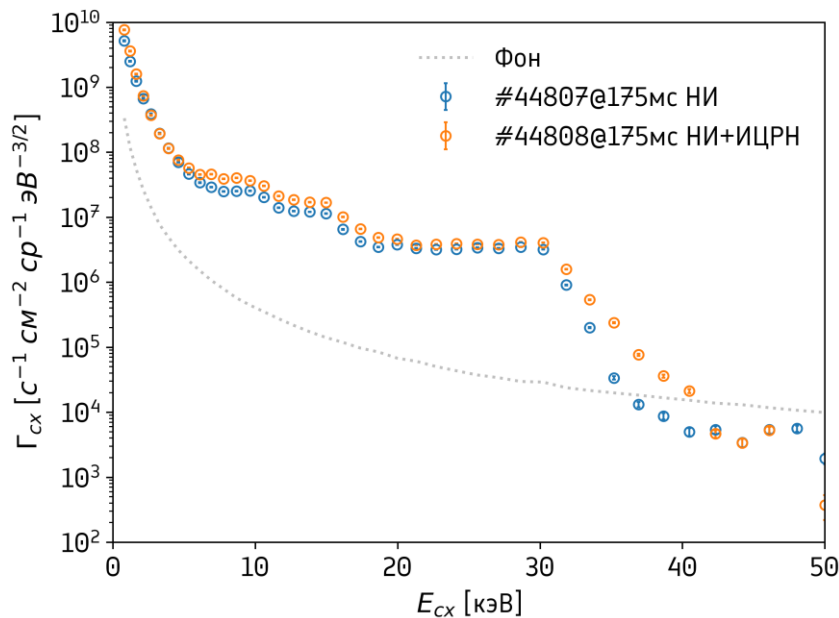
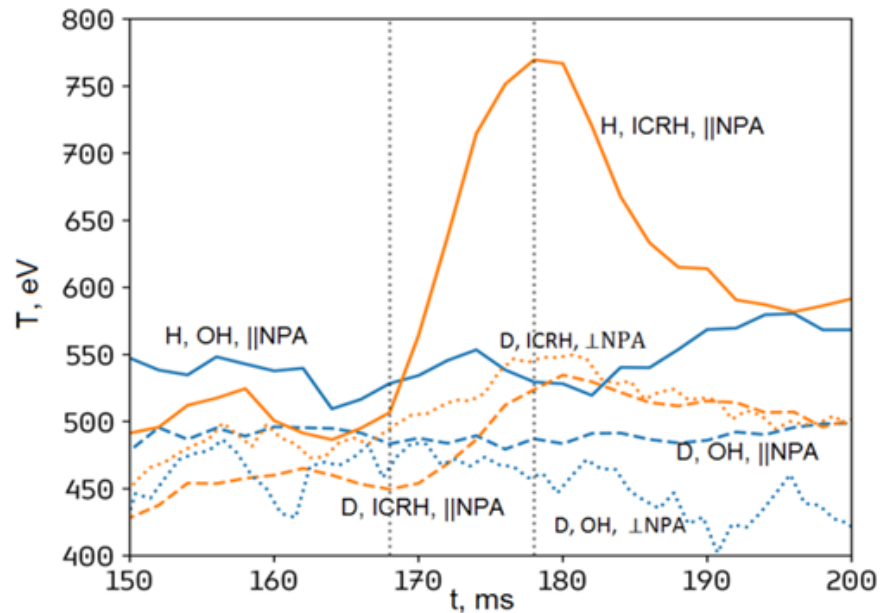
**Thank you
for your attention!**

Confinement: ICRH



Globus-M/M2 is the only ST successfully implementing Ion Cyclotron Resonance Heating

~100 kW ICRH

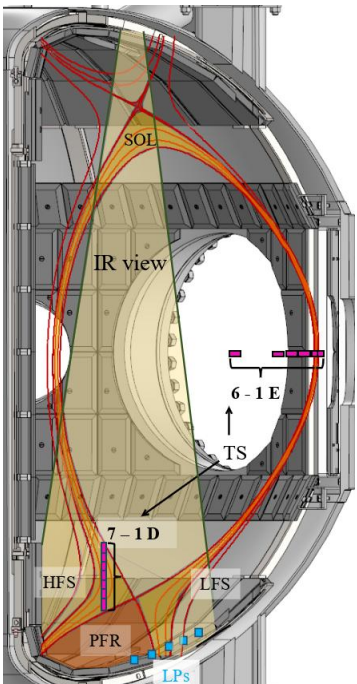


New Diagnostics: DTS

Divertor Thomson Scattering – prototyping ITER equipment

Diagnostics: [ERMAKOV, N. V., et al., Plasma Phys. Rep. 49 12 (2023) 1480]

Application: [MUKHIN E.E. EX-D, P2]

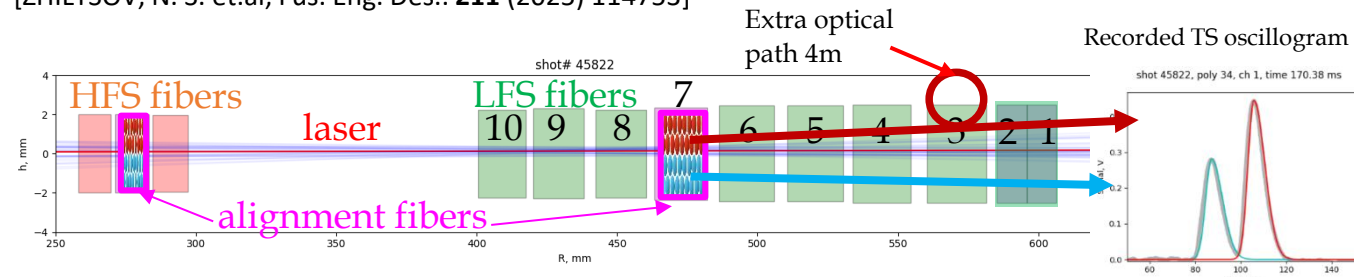


$T_e : 1\text{--}100 \text{ eV}$
 $n_e : 10^{17}\text{--}10^{20} \text{ m}^{-3}$
9 spatial points
resolution $\sim 1 \text{ cm}$,

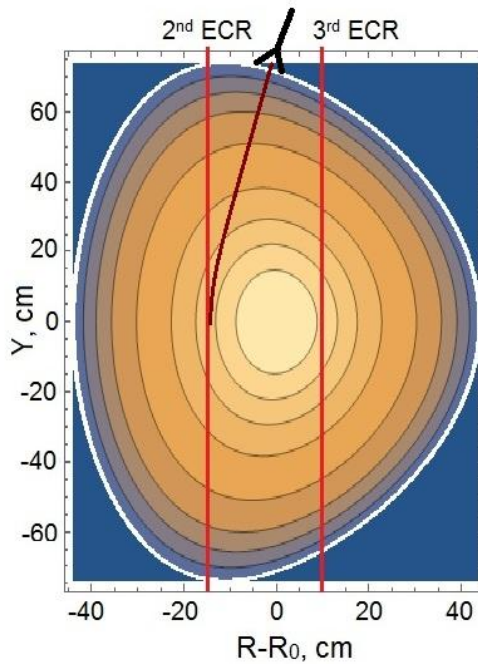
Applicability of the TS hardware in the tokamak control system was demonstrated: $\Delta\tau < 1 \text{ ms}$.
[ZHILTSOV, N. S. et al. Tech. Phys. Lett., **49** 8 (2023) 350-354.]

Precise ($\sim 0.1 \text{ mm}$) online alignment of the TS diagnostics was implemented in the equatorial TS.

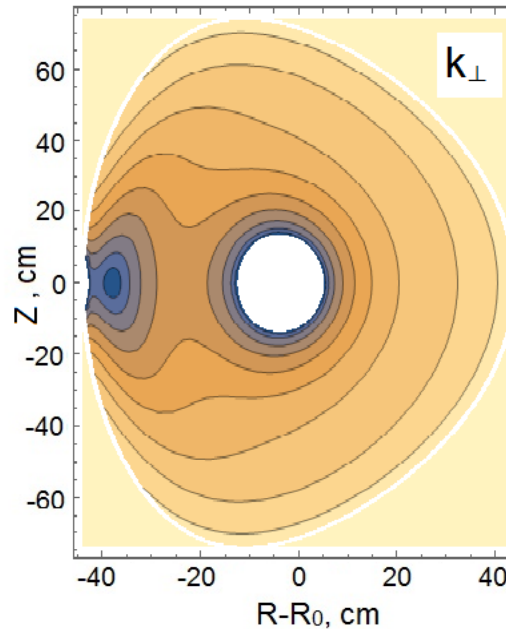
[ZHILTSOV, N. S. et.al, Fus. Eng. Des.. **211** (2025) 114753]



Globus-3



X2-mode



The ray-traced trajectory of the extraordinary wave is shown by the brown curve in the poloidal cross-section of Globus-3 ($n_0 = 1 \times 10^{20} \text{ m}^{-3}$, $T_e = 3 \text{ keV}$, $B_0 = 1.5 \text{ T}$) and (b) the contour diagram of the perpendicular component of the wave number of an extraordinary wave in the poloidal cross-section of Globus-3. The white region is the evanescence region due to the L-cutoff for the X-mode.

Conclusion



Advanced diagnostics and control were successfully implemented, including an Divertor Thomson Scattering system and fission chambers using ITER technologies and Laser Induced Ablation–Quadrupole Mass Spectrometer / Breakdown Spectroscopy.

A novel Inter-Shot Boronization technique was successfully developed and deployed, demonstrating advantage over standard GDB, leading to a significant reduction in plasma impurities ($Z_{\text{eff}} < 1.1$) and doubling of the neutron yield.

A hot-ion mode was established as a natural regime for Globus-M2. Deuterium NBI provides superior ion thermal insulation (close to neoclassical) compared to Hydrogen NBI, achieved through toroidal rotation gradient stabilization of ITG turbulence, resulting in higher ion temperatures (up to 4.7 keV) and energy confinement times.

ICRH experiments demonstrated 15% T_i increase and beam ions acceleration.

The **High-Field-Side High-Density phenomenon was identified for the first time in a spherical tokamak.**

Alfvén eigenmodes cause up to $\sim 30 \text{ MW/m}^2$ wall load, with losses explained by resonant convective transport of fast ions from the plasma core. For the first time fast ion transport and losses induced by EPM were observed.

A comprehensive study of edge instabilities was performed:

Small ELMs were shown to perturb plasma parameters outside the LCFS and cause fast particle losses.

Low triangularity destabilizes peeling-balloonning modes, leading to ELMs at lower pedestal pressures.

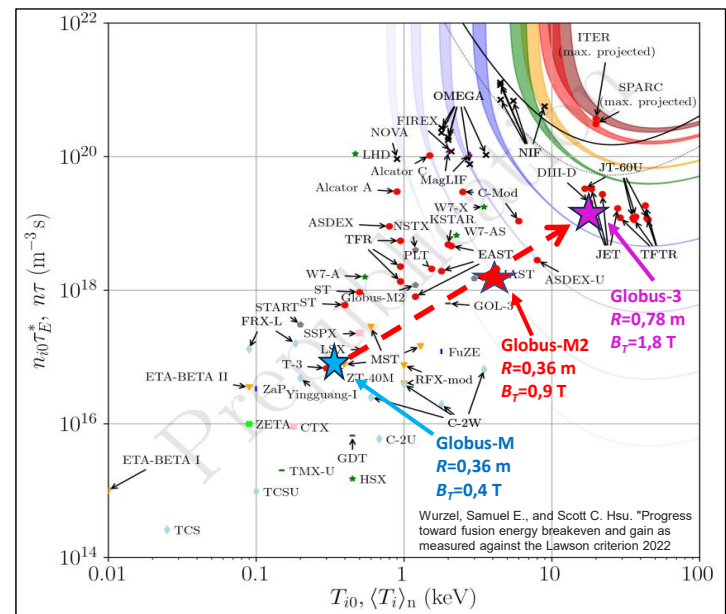
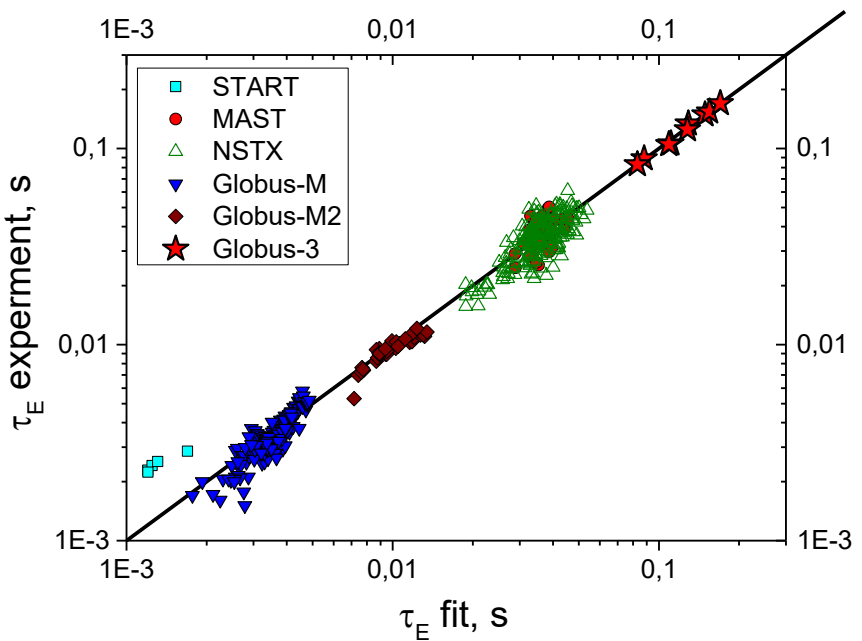
EHO were observed in ELM-free regimes.

The next-generation Globus-3 ST is under preliminary design. With significantly increased magnetic field (2 T), major radius (0.775 m), and plasma current (up to 2 MA), it is projected to achieve **fusion-relevant ion temperatures** and study alpha-particle physics from the $p + {}^{11}\text{B}$ reaction.

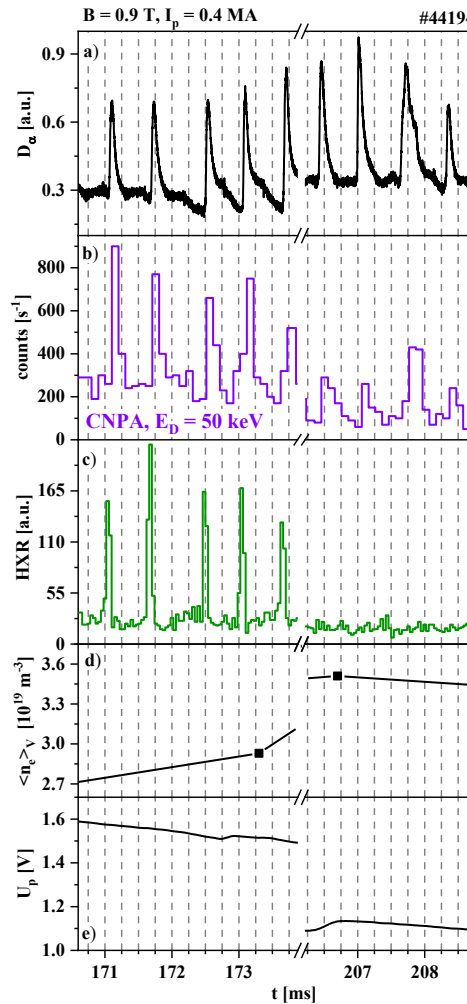
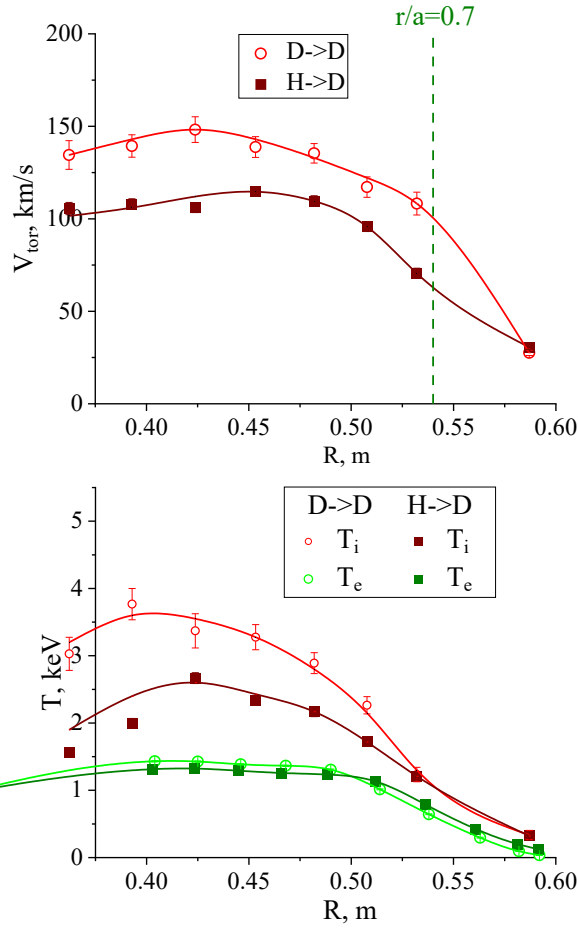


Globus-3

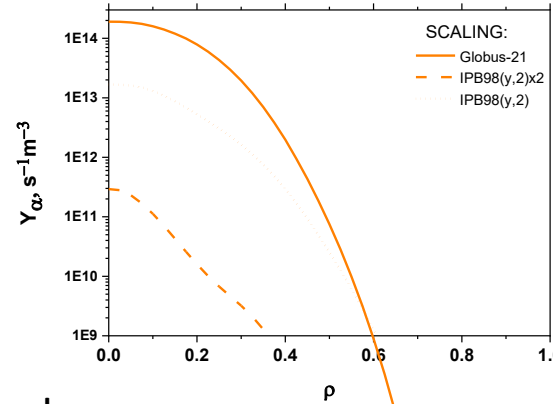
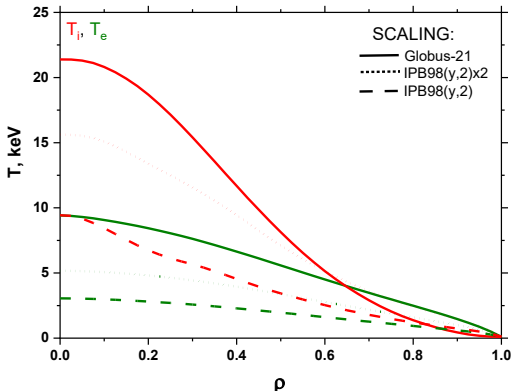
$$\tau_E^{Globus-21} = 0,066 \cdot I_p^{0.53} \cdot B_T^{1.05} \cdot P_{abs}^{-0.58} \cdot n_e^{0.65} \cdot R^{2.66} \cdot \kappa^{0.78}$$



Scaling suggests the importance of B_T increase. Will be tested at Globus-3.



Thermoneuclear reaction



Beam-plasma

